Nonlinear Dyn (2022) 109:2281–2295
https://doi.org/10.1007/s11071-022-07589-y

ORIGINAL PAPER

Stochastic response determination of U-OWC energy harvesters: a statistical linearization solution treatment accounting for intermittent wave excitation

Andrea Scialò · Giovanni Malara · Ioannis A. Kougioumtzoglou · Felice Arena

Received: 18 November 2021 / Accepted: 23 May 2022 / Published online: 29 June 2022

Abstract A novel statistical linearization technique is developed for determining approximately the response statistics and the power output of U-Oscillating Water Column (U-OWC) energy harvesting systems. In this regard, first, the governing equations are derived by employing the unsteady Bernoulli equation. Note that the intermittent, i.e., non-stationary, nature of the wave excitation, occurring in severe sea states due to uncovering of the U-OWC inlet, is explicitly accounted for in the herein proposed model. This is done by multiplying the excitation process with a Heaviside function dependent on the instantaneous free surface displacement. Next, the resulting coupled system of nonlinear integro-differential stochastic equations is solved approximately by relying on a statistical linearization technique. Specifically, the original system of nonlinear equations is replaced by an equivalent linear one, whose parameters and response first- and second-order statistics are obtained by minimizing the mean square error between the two systems. A significant novel aspect of the technique relates to the fact that the Heaviside function is replaced in the equivalent linear system by an "equivalent excitation" coefficient to be determined as part of the statistical linearization solution scheme. Further, compared with other relevant solution schemes adopted in earlier research efforts in the literature, it is shown that the developed technique can be construed as a direct generalization that exhibits an enhanced accuracy degree. The U-OWC installed in the Civitavecchia harbor (Rome, Italy) is considered as an illustrative numerical example, where the reliability of the approximate technique is demonstrated by comparisons with pertinent Monte Carlo simulation data.

Keywords Renewable energy · Wave energy · Oscillating water column · U-OWC · Statistical linearization · Monte Carlo

A. Scialò · G. Malara · F. Arena (✉)
Natural Ocean Engineering Laboratory - DICEAM, "Mediterranea" University of Reggio Calabria, Loc. Feo di Vito, 89122 Reggio Calabria, Italy
e-mail: arena@unirc.it

A. Scialò
e-mail: andrea.scialo@unirc.it

G. Malara
e-mail: giovanni.malara@unirc.it

I. A. Kougioumtzoglou
Department of Civil Engineering and Engineering Mechanics, Columbia University, 500 W. 120th Street, New York, NY 10027, USA
e-mail: ikougioum@columbia.edu

1 Introduction

The increasing demand for electricity consumption, in conjunction with government policies fostering CO_2 reduction, is currently urging industry and academia to develop efficient devices for harvesting energy from renewable sources. In this context, wave energy has upgraded its role in the renewable energy sector, primarily by virtue of its abundant distribution both nearshore and offshore. Further, a number of wave

energy converters (WECs) have been designed and tested to date with varying degrees of success [1]. Among them, oscillating water columns (OWCs) have proved to be reliable, efficient and versatile, as they can be easily integrated into vertical breakwaters [2], or into floating multi-purpose platforms [3], thus reducing the associated construction cost. OWCs comprise a semi-submerged hollow chamber with a vertical opening located below the mean water level, which is exposed directly to sea waves. The waves induce oscillations of the water column inside the chamber. Consequently, the air trapped in the upper part of the chamber is alternately compressed and expanded. This creates an air flow through a self-rectifying air turbine, such as the Wells [4] or the biradial turbines [5]. During the last decade, OWCs have been widely studied with the aim to enhance their performance and maximize the harvested energy. This effort has led to testing various geometrical configurations, such as OWCs with an artificial step at the front sea bottom [6], or L-shaped OWCs [7].

In this work, the U-OWC configuration is considered [8]. This OWC converter has a U-shaped duct, which increases the inertia of the converter and places the opening of the device close to the mean water level. This ensures that the U-OWC natural frequency can be tuned over a wide frequency range, which leads to increased energy harvesting compared to a traditional OWC [9]. In fact, this was further corroborated by pertinent experiments in Ref. [10], where it was shown that the U-OWC configuration exhibited enhanced hydrodynamic performance compared to the traditional OWC, or to the L-shaped OWC. Moreover, the performance of the U-OWC is strongly dependent on its geometrical characteristics [11,12], such as the length and the width of the U-duct, the position of its opening below the mean water level, and the width and height of the inner chamber. Further, the optimal selection and control of the Power Take-Off (PTO) system is critical for maximizing the amount of converted energy [13]. In this regard, note that various alternatives to self-rectifying turbines are currently emerging [14].

As far as the theoretical model describing the U-OWC dynamics is concerned, a basic formulation was first proposed by Boccotti [15] that was subsequently refined by Malara et al. [16] to account for previously neglected memory effects. Specifically, the U-OWC dynamics is described by the unsteady Bernoulli equation. The resulting U-OWC nonlinear integro-differential equation is coupled to the air mass conservation equation as applied to the air chamber volume under the assumption of an isentropic thermodynamic process. As anticipated due to the nonlinear terms in the governing equation, the system is not amenable to an analytical solution treatment, and thus, alternative numerical approaches are typically employed for determining response statistics and, eventually, for optimizing the U-OWC (e.g., [15]). Nevertheless, brute-force numerical solution schemes, such as standard implementations of Monte Carlo (MC) simulation, can be computationally prohibitive. In this regard, versatile and computationally efficient approximate stochastic dynamics methodologies, such as the potent Wiener path integral (WPI) technique (e.g., [17,18]), appear capable of treating diverse energy harvesting systems. Indicatively, the WPI technique has been successfully utilized recently for stochastic response determination and design optimization of a certain class of nonlinear electro-mechanical energy harvesters [19,20].

Further, statistical linearization has been one of the most versatile methodologies in stochastic dynamics for determining, accurately and in a computationally efficient manner, first- and second-order response statistics of nonlinear systems; see [21,22] for a broad perspective. In passing, it is worth noting recent generalizations and extensions of statistical linearization to account for joint time-frequency response analysis (e.g., [23]), for fractional derivative modeling (e.g., [24]), as well as for systems with singular parameter matrices (e.g., [25]). Furthermore, statistical linearization has been employed for stochastic response determination and optimization of diverse wave energy harvesting devices [26], including point-absorbers [27], OWCs [28], and arrays of OWCs and U-OWCs [29]. Also, the methodology has found practical applications pertaining, indicatively, to the case study of the U-OWC in the Civitavecchia harbor (Rome, Italy) [30], and to the design of a U-OWC wave power plant to be installed in the Mediterranean Sea [11]. Although statistical linearization has exhibited a high degree of reliability in determining both OWC and U-OWC statistics, note that the horizontal opening of the U-duct is closer to the free surface compared to the traditional OWCs. Thus, the system can be exposed to intermittent wave excitation. That is, the U-OWC inlet uncovers itself during the crossing of large wave troughs. Clearly, this phenomenon is quite rare in low-energy sea states. However, it becomes quite frequent in cases of severe seas, where the system is exposed to rela-

tively large waves. Note that the position of the vertical duct opening affects the hydrodynamic efficiency of the harvester. Specifically, if it is quite deep, the magnitude of the applied wave pressure is small. If it is quite close to the mean water level, the water column inlet uncovers itself frequently, resulting in a considerable loss of energy to be harvested. In this regard, considering time domain response analyses within the context of a MC solution treatment of the problem, the above phenomenon can be readily taken into account by examining at a given time instant whether the water surface is below, or not, the U-duct opening. Nevertheless, referring to earlier efforts considering a statistical linearization solution treatment of the problem, the inlet uncovering effect was either neglected [29,30], or accounted for in a rather heuristic manner [11]. In both cases, it is clear that the degree of the involved approximations is quite high, especially in cases of severe seas where inlet uncovering can be a frequent event.

In this paper, a novel statistical linearization technique is developed for determining the stochastic response of U-OWC systems. Specifically, the developed technique accounts explicitly for the effect of intermittent, i.e., non-stationary, wave excitation occurring in energy-wise rich seas. This is done, first, by multiplying the excitation process with a Heaviside function dependent on the instantaneous free surface displacement. Next, the Heaviside function is replaced in the equivalent linear system by a novel "equivalent excitation" coefficient to be determined as part of the statistical linearization technique. In this regard, the technique can be construed as a generalization and enhancement of the solution approach proposed in [29,30] to significantly improve the exhibited accuracy degree. The reliability of the technique is demonstrated by comparisons with pertinent MC simulation data relating to the U-OWC installed in the Civitavecchia harbor [31].

2 U-Oscillating water column governing equations

The water column oscillations are described by the unsteady Bernoulli equation, which is formulated by enforcing the energy balance principle between two sections of the water column: one section is located at the U-duct opening; and the other one at the instantaneous free surface in the inner chamber, as shown in Fig. 1. Thus, considering a U-OWC installed at a

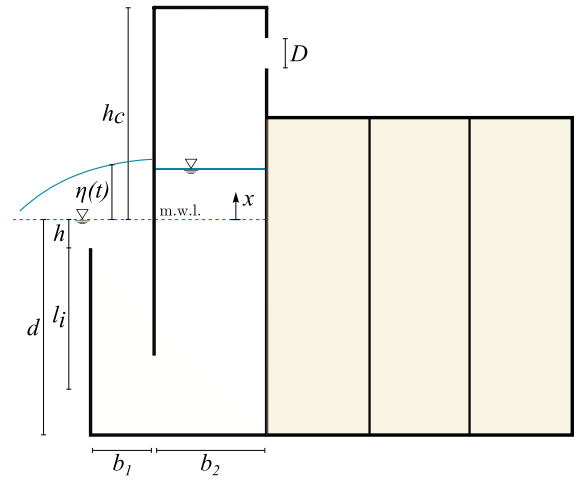

Fig. 1 U-OWC cross section

water depth d, with U-duct length and width l_i and b_1, respectively, chamber width b_2, and inlet submergence with respect to the mean water level h, the following governing equation is obtained (see also [16]), i.e.,

$$\begin{aligned}
&\left[\frac{1+C_\mathrm{in}}{g}\left(\frac{b_2}{b_1}\,l_\mathrm{i}+l_\mathrm{i}+h+x\right)+\frac{b_2}{gb_1}\,H_\infty\right]\ddot{x}\\
&\quad+\frac{1}{2g}\left[C_\mathrm{dg}\left(\frac{l_\mathrm{i}}{R_\mathrm{h1}}\left(\frac{b_2}{b_1}\right)^2+\frac{l_\mathrm{i}+h+x}{R_\mathrm{h2}}\right)\,|\,\dot{x}\,|\right]\dot{x}\\
&\quad+\left[1-\left(\frac{b_2}{b_1}\right)^2\right]\frac{\dot{x}^2}{2g}+x+\frac{p_\mathrm{c}-p_\mathrm{atm}}{\rho g}\\
&\quad+\frac{b_2}{gb_1}\int_{-\infty}^{t}K(t-\tau)\,\dot{x}(\tau)\mathrm{d}\tau=\frac{\Delta p^{(D)}}{\rho g}.
\end{aligned}\tag{1}$$

In Eq. (1), $x(t)$ is the instantaneous water column displacement, positive upward and measured from the mean water level; g is the acceleration due to gravity; ρ is the water density; C_dg and C_in are coefficients derived through experimental data accounting for continuous head losses [31]; H_∞ is a length accounting for the infinite frequency added mass; $K(t)$ is the retardation function accounting for memory effects; p_c and p_atm are the air pressure in the chamber and the atmospheric pressure, respectively; $\Delta p^{(D)}$ is the excitation pressure computed at the centre of the U-duct opening in a diffracted wave field; and R_h1 and R_h2 are the hydraulic radii given by the equations

$$R_{h1} = \frac{b_1 b_3}{2(b_1 + b_3)}, \tag{2}$$

and

$$R_{h2} = \frac{b_2 b_3}{2(b_2 + b_3)}, \tag{3}$$

with b_3 being the transverse width of the chamber.

Next, denoting the terms in square brackets on the left-hand side of Eq. (1) as

$$M(x) = \left[\frac{1 + C_{in}}{g} \left(\frac{b_2}{b_1} l_i + l_i + h + x \right) + \frac{b_2}{g b_1} H_\infty \right], \tag{4}$$

and

$$C(x, \dot{x}) = \frac{1}{2g} \left[C_{dg} \left(\frac{l_i}{R_{h1}} \left(\frac{b_2}{b_1} \right)^2 + \frac{l_i + h + x}{R_{h2}} \right) \mid \dot{x} \mid \right] + \left[1 - \left(\frac{b_2}{b_1} \right)^2 \right] \frac{\dot{x}}{2g}, \tag{5}$$

and introducing the Heaviside step function $H(t)$ [32], defined as

$$H(t) = \begin{cases} 1 & \text{if } t > 0 \\ 0 & \text{if } t < 0 \end{cases}, \tag{6}$$

the equation describing the water column oscillations takes the form

$$M(x)\ddot{x} + C(x, \dot{x})\dot{x} + x + \frac{p_c - p_{atm}}{\rho g} + \frac{b_2}{g b_1} \int_{-\infty}^{t} K(t - \tau)\, \dot{x}(\tau) d\tau = \frac{\Delta p^{(D)}}{\rho g} H(\eta(t) + h), \tag{7}$$

where η represents the instantaneous free surface displacement at the U-OWC inlet.

Comparing Eq. (1) with Eq. (7), it is seen that the latter incorporates also the inlet uncovering effect by enforcing a zero excitation value when the free surface displacement $\eta(t)$ is smaller than $-h$. This enhanced modeling reflects the fact that the inlet is directly exposed to the atmosphere when the free surface displacement is below the U-OWC opening. Thus, there is no wave excitation. Note that a consistent application of this approach dictates a similar treatment also for H_∞ and for certain values of the convolution integral as they are elements of the wave field representation, and thus, of the wave pressure calculation (see Ref. [16] for a detailed description of the mathematical formulation). Nevertheless, its use is limited herein to the system excitation only. This yields a more sophisticated and realistic modeling of the problem, without unnecessarily complicating further the governing equation and rendering it possibly intractable from a solution treatment perspective. In fact, noticing that H_∞ is small compared to the total mass $M(x)$, and that the hydrodynamic memory computation usually spans a time window larger than typical individual wave periods, provides a reasonable justification of the aforementioned modeling.

Further, Eq. (7) is coupled to the air chamber equation, which is obtained by considering an isentropic process for the compression and expansion phases [33], and by relying on the mass conservation principle; this yields (see also Ref. [16])

$$b_2 b_3 (h_c - x)\, \dot{p}_c - \gamma b_2 b_3 p_c \dot{x} + \gamma p_c \left(\frac{p_{atm}}{p_c} \right)^{1/\gamma} \frac{\dot{m}_{turb}}{\rho_{atm}} = 0, \tag{8}$$

where h_c is the air chamber height above the mean water level; γ is the specific heat ratio; ρ_{atm} is the air density in the atmosphere; and $\dot{m}_{turb}$ is the air mass flow rate through the turbine (positive for outward flows) given by the equation

$$\dot{m}_{turb} = \frac{\Lambda D}{\Omega} (p_c - p_{atm}). \tag{9}$$

Equation (9) pertains to Wells turbines, where Λ is the dimensionless turbine coefficient depending on the turbine geometry [34], D is the turbine outer diameter and Ω is the turbine rotational speed. Next, defining

$$C_p(x) = b_2 b_3 (h_c - x), \tag{10}$$

$$C_x(p_c) = -\gamma b_2 b_3 p_c \tag{11}$$

and

$$K_p(p_c) = \gamma \left(\frac{p_{atm}}{p_c} \right)^{1/\gamma} \frac{\dot{m}_{turb}}{\rho_{atm}}, \tag{12}$$

Equation (8) becomes

$$C_p(x)\, \dot{p}_c + C_x(p_c)\, \dot{x} + K_p(p_c)\, p_c = 0. \tag{13}$$

3 Statistical linearization solution

In this section, a novel statistical linearization technique is developed for determining the stochastic response of U-OWC systems, which can be construed as a generalization and enhancement of the solution approach proposed in [29,30] to significantly improve the exhibited accuracy degree.

Specifically, Eqs. (7) and (13) form a coupled system of nonlinear integro-differential equations with no closed-form solution. According to the standard statistical linearization formulation [21], the original system of nonlinear equations is approximated by an equivalent linear one, whose parameters are obtained by minimizing the mean square error between the two systems. Considering the fact that the nonlinear terms are asymmetric, an offset in the system response must be also included [35]. Therefore, the system response is represented through the sum of a zero mean random process and a constant mean value as

$$x = x_0 + m_{\rm x}, \tag{14}$$

and

$$\Delta p_{\rm c} = \Delta p_0 + m_{\rm p}, \tag{15}$$

where $\Delta p_{\rm c} = p_{\rm c} - p_{\rm atm}$; x_0 and Δp_0 are the zero-mean random components of the oscillating water column displacement and air pressure, respectively, and $m_{\rm x}$ and $m_{\rm p}$ are the mean values of the response components. Utilizing eqs. (14)–(15), the U-OWC governing eqs.(7) and (13) becomes, respectively,

$$\begin{aligned} &M\ddot{x}_0 + \frac{1+C_{\rm in}}{g} x_0\ddot{x}_0 + \\ &\frac{1}{2g}\left[C_{\rm dg}\left(\frac{l_{\rm i}}{R_{\rm h1}}\left(\frac{b_2}{b_1}\right)^2 + \frac{l_{\rm i}+h+x_0+m_{\rm x}}{R_{\rm h2}}\right)\right]|\dot{x}_0|\,\dot{x}_0 + \\ &\left[1-\left(\frac{b_2}{b_1}\right)^2\right]\frac{\dot{x}_0^2}{2g} + \frac{1}{g}\frac{b_2}{b_1}\int_{-\infty}^{t} K(t-\tau)\dot{x}_0(\tau)\,{\rm d}\tau \\ &+ x_0 + m_{\rm x} + \frac{\Delta p_0}{\rho g} + \frac{m_{\rm p}}{\rho g} = \frac{\Delta p^{(\rm D)}}{\rho g} H(\eta(t)+h), \end{aligned} \tag{16}$$

and

$$\begin{aligned} &C_{\rm p}^{(2)}\Delta\dot{p}_0 - b_2b_3x_0\Delta\dot{p}_0 + C_{\rm x}^{(2)}\dot{x}_0 - \gamma b_2b_3\Delta p_0\dot{x}_0 + \\ &\gamma(\Delta p_0 + m_{\rm p} + p_{\rm atm})\left(\frac{p_{\rm atm}}{\Delta p_0 + m_{\rm p} + p_{\rm atm}}\right)^{\frac{1}{\gamma}}\frac{\dot{m}_{\rm turb}}{\rho_{\rm atm}} = 0, \end{aligned} \tag{17}$$

where M, $C_{\rm p}^{(2)}$ and $C_{\rm x}^{(2)}$ are given by

$$M = \left[\frac{1+C_{\rm in}}{g}\left(\frac{b_2}{b_1}\,l_{\rm i} + l_{\rm i} + h + m_{\rm x}\right) + \frac{b_2}{gb_1}\,H_\infty\right], \tag{18}$$

$$C_{\rm p}^{(2)} = b_2b_3\,(h_{\rm c} - m_{\rm x})\,, \tag{19}$$

and

$$C_{\rm x}^{(2)} = -\gamma b_2b_3\left(m_{\rm p} + p_{\rm atm}\right). \tag{20}$$

Next, the equivalent linear system is given by the set of equations

$$\begin{aligned} &(M + M_{\rm eq}^{(1)})\ddot{x}_0 + C_{\rm eq}^{(1)}\dot{x}_0 + \frac{1}{g}\frac{b_2}{b_1}\int_{-\infty}^{t} K(t-\tau)\dot{x}_0(\tau)\,{\rm d}\tau \\ &\quad + (1 + K_{\rm eq}^{(1)})x_0 + \frac{\Delta p_0}{\rho g} = \beta_{\rm eq}\frac{\Delta p^{(\rm D)}}{\rho g}, \end{aligned} \tag{21}$$

and

$$\begin{aligned} &\left(C_{\rm p}^{(2)} + C_{\rm p,eq}^{(2)}\right)\Delta\dot{p}_0 + \left(C_{\rm x}^{(2)} + C_{\rm x,eq}^{(2)}\right)\dot{x}_0 \\ &\quad + K_{\rm p,eq}^{(2)}\Delta p_0 + K_{\rm x,eq}^{(2)}x_0 = 0, \end{aligned} \tag{22}$$

where $M_{\rm eq}^{(1)}$, $C_{\rm eq}^{(1)}$, $K_{\rm eq}^{(1)}$, β_{eq}, $C_{\rm p,eq}^{(2)}$, $C_{\rm x,eq}^{(2)}$, $K_{\rm p,eq}^{(2)}$, and $K_{\rm x,eq}^{(2)}$ are the unknown coefficients to be determined by the mean square error minimization procedure.

Note that a significant novel aspect of Eq. (21) pertains to the consideration of the coefficient β_{eq} corresponding to an "equivalent excitation." This was not included in previous models [29,30]. The rationale relates to the fact that the herein proposed modeling accounts explicitly for the effect of intermittent, i.e., non-stationary, wave excitation occurring in energy-wise rich seas. This is done by multiplying the excitation process on the right-hand side of Eq. (7) with a Heaviside function dependent on the instantaneous free surface displacement. In this regard, the Heaviside function is treated as a nonlinear term to be replaced by an equivalent excitation coefficient, which is calculated as part of the statistical linearization technique. Note that compared to earlier efforts in the literature [29,30], the herein developed statistical linearization solution treatment yielding the additional coefficient $\beta_{\rm eq}$ can be construed as a generalization toward accuracy enhancement.

To elaborate further and provide some additional insight, note that the Heaviside function $H(\eta(t)+h)$ depends implicitly on the response velocity $\dot{x}$. This is

due to the fact that according to the linear potential flow theory [36], the free surface displacement $\eta(t)$ is the superposition of a diffracted free surface and a radiated free surface $\eta_r(t)$ dependent on $\dot{x}$. Indeed, the $\dot{x}-\eta$ relationship is an established result of the linear water wave theory. Specifically, the equation representing the radiated waves takes the form

$$\eta_r(t) = \int_0^{+\infty} K_\eta(\tau)\dot{x}(t-\tau)\,\mathrm{d}\tau. \tag{23}$$

In this regard, the term $\frac{\Delta p^{(D)}}{\rho g}H(\eta(t)+h)$ on the right-hand side of Eq. (16) can be construed, alternatively, as a nonlinear parametric stochastic excitation term; see also [37] for a similar interpretation of parametric excitation as "equivalent external excitation." In fact, it is remarked that second-order response statistics of structural systems with nonlinear parametric stochastic excitation terms were determined in [38] based on a statistical linearization treatment, which is somewhat similar to the herein developed technique.

Further, the mean square error to be minimized is given by the equation

$$E[\varepsilon^2] = E[\varepsilon_1^2 + \varepsilon_2^2], \tag{24}$$

where $E[\cdot]$ denotes the mathematical expectation operator;

$$\begin{aligned}\varepsilon_1 = {} & \frac{1+C_{in}}{g}x_0\ddot{x}_0 + \frac{1}{2g}\left[C_{dg}\left(\frac{l_i}{R_{h1}}\left(\frac{b_2}{b_1}\right)^2 + \frac{l_i+h+x_0+m_x}{R_{h2}}\right)\right]|\dot{x}_0|\,\dot{x}_0 \\ & + \left[1-\left(\frac{b_2}{b_1}\right)^2\right]\frac{\dot{x}_0^2}{2g} + m_x + \frac{m_p}{\rho g} \\ & - \frac{\Delta p^{(D)}}{\rho g}H(\eta(t)+h) - M_{eq}^{(1)}\ddot{x}_0 - C_{eq}^{(1)}\dot{x}_0 \\ & - K_{eq}^{(1)}x_0 + \frac{\Delta p^{(D)}}{\rho g}\beta_{eq};\end{aligned} \tag{25}$$

and

$$\begin{aligned}\varepsilon_2 = {} & -b_2b_3x_0\Delta\dot{p}_0 - \gamma b_2b_3\Delta p_0\dot{x}_0 \\ & + \gamma(\Delta p_0 + m_p + p_{atm})\left(\frac{p_{atm}}{\Delta p_0 + m_p + p_{atm}}\right)^{\frac{1}{\gamma}} \\ & \times \frac{\dot{m}_{turb}}{\rho_{atm}} - C_{p,eq}^{(2)}\Delta\dot{p}_0 - C_{x,eq}^{(2)}\dot{x}_0 - K_{p,eq}^{(2)}\Delta p_0 \\ & - K_{x,eq}^{(2)}x_0.\end{aligned} \tag{26}$$

Next, applying the minimization criterion to Eq. (24) yields the following set of equations to be solved for obtaining the optimization unknowns, i.e.,

$$\begin{aligned}\frac{\partial}{\partial M_{eq}^{(1)}}E[\varepsilon^2] &= \frac{\partial}{\partial C_{eq}^{(1)}}E[\varepsilon^2] \\ &= \frac{\partial}{\partial K_{eq}^{(1)}}E[\varepsilon^2] = \frac{\partial}{\partial \beta_{eq}}E[\varepsilon^2] \\ &= \frac{\partial}{\partial C_{p,eq}^{(2)}}E[\varepsilon^2] = \frac{\partial}{\partial C_{x,eq}^{(2)}}E[\varepsilon^2] = \frac{\partial}{\partial K_{p,eq}^{(2)}}E[\varepsilon^2] \\ &= \frac{\partial}{\partial K_{x,eq}^{(2)}}E[\varepsilon^2] = 0.\end{aligned} \tag{27}$$

The equations for obtaining the equivalent coefficients are derived by employing Eqs. (25)–(26) and expanding Eq. (27) for each one of the unknown terms. That is, by taking the derivative of the mean square error with respect to $M_{eq}^{(1)}$, $C_{eq}^{(1)}$, $K_{eq}^{(1)}$, β_{eq}, $C_{p,eq}^{(2)}$, $C_{x,eq}^{(2)}$, $K_{p,eq}^{(2)}$, and $K_{x,eq}^{(2)}$. This procedure leads to a system of eight equations, which are reported in the following in the form of three sub-systems, i.e.,

$$\begin{aligned}&\begin{bmatrix} \sigma_{\ddot{x}_0}^2 & E[x_0\ddot{x}_0] & -E\left[\ddot{x}_0\frac{\Delta p^{(D)}}{\rho g}\right] \\ E[x_0\ddot{x}_0] & \sigma_{x_0}^2 & -E\left[x_0\frac{\Delta p^{(D)}}{\rho g}\right] \\ -E\left[\ddot{x}_0\frac{\Delta p^{(D)}}{\rho g}\right] & -E\left[x_0\frac{\Delta p^{(D)}}{\rho g}\right] & \sigma_{\frac{\Delta p^{(D)}}{\rho g}}^2 \end{bmatrix}\begin{bmatrix} M_{eq}^{(1)} \\ K_{eq}^{(1)} \\ \beta_{eq}\end{bmatrix} \\ &= \begin{bmatrix} -E\left[\frac{\Delta p^{(D)}}{\rho g}H(\eta(t)+h)\ddot{x}_0\right] \\ -E\left[\frac{\Delta p^{(D)}}{\rho g}H(\eta(t)+h)x_0\right] \\ E\left[\left(\frac{\Delta p^{(D)}}{\rho g}\right)^2 H(\eta(t)+h)\right]\end{bmatrix},\end{aligned} \tag{28}$$

$$\begin{aligned}C_{eq}^{(1)} = {} & \frac{1}{2g}\left[C_{dg}\left(\frac{l_i}{R_{h1}}\left(\frac{b_2}{b_1}\right)^2 + \frac{l_i+h+m_x}{R_{h2}}\right)\right] \\ & \frac{E\left[|\dot{x}_0|\,\dot{x}_0^2\right]}{\sigma_{\dot{x}_0}^2} - \frac{E\left[\frac{\Delta p^{(D)}}{\rho g}H(\eta(t)+h)\dot{x}_0\right]}{\sigma_{\dot{x}_0}^2},\end{aligned} \tag{29}$$

and

$$\begin{bmatrix} \sigma^2_{\dot{\Delta}p_0} & E\left[\dot{x}_0\dot{\Delta}p_0\right] & 0 & E\left[x_0\dot{\Delta}p_0\right] \\ E\left[\dot{x}_0\dot{\Delta}p_0\right] & \sigma^2_{\dot{x}_0} & E\left[\Delta p_0\dot{x}_0\right] & 0 \\ 0 & E\left[\dot{x}_0\Delta p_0\right] & \sigma^2_{\Delta p_0} & E\left[x_0\Delta p_0\right] \\ E\left[x_0\dot{\Delta}p_0\right] & 0 & E\left[x_0\Delta p_0\right] & \sigma^2_{x_0} \end{bmatrix} \begin{bmatrix} C^{(2)}_{\mathrm{p,eq}} \\ C^{(2)}_{\mathrm{x,eq}} \\ K^{(2)}_{\mathrm{p,eq}} \\ K^{(2)}_{\mathrm{x,eq}} \end{bmatrix} =$$

$$\begin{bmatrix} 0 \\ \gamma\left(\frac{p_{\mathrm{atm}}}{\rho_{\mathrm{atm}}}\right)^{1/\gamma} E\left[\dot{m}_{\mathrm{turb}}\left(\Delta p_0 + m_{\mathrm{p}} + p_{\mathrm{atm}}\right)^{\left(1-\frac{1}{\gamma}\right)}\dot{x}_0\right] \\ \gamma\left(\frac{p_{\mathrm{atm}}}{\rho_{\mathrm{atm}}}\right)^{1/\gamma} E\left[\dot{m}_{\mathrm{turb}}\left(\Delta p_0 + m_{\mathrm{p}} + p_{\mathrm{atm}}\right)^{\left(1-\frac{1}{\gamma}\right)}\Delta p_0\right] \\ \gamma\left(\frac{p_{\mathrm{atm}}}{\rho_{\mathrm{atm}}}\right)^{1/\gamma} E\left[\dot{m}_{\mathrm{turb}}\left(\Delta p_0 + m_{\mathrm{p}} + p_{\mathrm{atm}}\right)^{\left(1-\frac{1}{\gamma}\right)}x_0\right] \end{bmatrix}, \quad (30)$$

where the σ^2 denotes the variance of a random process. Compared to earlier relevant efforts in the literature [11,29], the proposed statistical linearization formulation leads to nonzero values of $M^{(1)}_{\mathrm{eq}}$ and $K^{(1)}_{\mathrm{eq}}$, which are determined in conjunction with the equivalent excitation coefficient β_{eq}. Remarkably, the herein developed solution methodology can be construed as a direct generalization of the results obtained in [11,29]. In fact, for the limiting case $H(\eta(t)+h) = 1$, Eq. (28) yields $M^{(1)}_{\mathrm{eq}} = 0$, $K^{(1)}_{\mathrm{eq}} = 0$, and $\beta_{eq} = 1$, which is precisely the modeling of the equivalent linear system adopted in [11,29].

Further, it is seen that the equivalent elements in Eqs. (28)–(30) depend on the unknown system response statistics, and therefore, additional equations need to be considered. In this regard, to derive input–output relationships, Eqs.(21)–(22) are transformed in the frequency domain and become

$$\left[-\omega^2\left(M + M^{(1)}_{\mathrm{eq}}\right) + i\omega C\mathrm{eq} + i\omega\frac{b_2}{gb_1}\widetilde{K}(\omega) + \left(1 + K^{(1)}_{\mathrm{eq}}\right)\right]\widetilde{X}(\omega) + \frac{1}{\rho g}\Delta\widetilde{p}_0(\omega) = \frac{1}{\rho g}\Delta\widetilde{p}^{(\mathrm{D})}(\omega)\beta_{\mathrm{eq}}, \quad (31)$$

and

$$\left[i\omega\left(C^{(2)}_{\mathrm{p}} + C^{(2)}_{\mathrm{p,eq}}\right) + K^{(2)}_{\mathrm{p,eq}}\right]\Delta\widetilde{p}_0(\omega) + \left[i\omega\left(C^{(2)}_{\mathrm{x}} + C^{(2)}_{\mathrm{x,e\,q}}\right) + K^{(2)}_{\mathrm{x,eq}}\right]\widetilde{X}(\omega) = 0. \quad (32)$$

$\widetilde{X}(\omega)$, $\Delta\widetilde{p}_0(\omega)$, $\Delta\widetilde{p}^{(\mathrm{D})}(\omega)$ and $\widetilde{K}(\omega)$ denote the Fourier transforms of x_0, Δp_0, $\Delta p^{(\mathrm{D})}(t)$ and $K(t)$, respectively.

Also, the mean values, m_{x} and m_{p}, are obtained by taking the expected values of the nonlinear equations (16) and (17). That is,

$$m_{\mathrm{x}} = -\frac{1 + C_{\mathrm{in}}}{g}E\left[x_0\ddot{x}_0\right] - \frac{m_{\mathrm{p}}}{\rho g} + E\left[\frac{\Delta p^{(D)}}{\rho g}H(\eta(t)+h)\right] - \frac{1}{2g}\left[1 - \left(\frac{b_2}{b_1}\right)^2\right]\sigma^2_{\dot{x}_0}, \quad (33)$$

and

$$-b_2b_3E\left[x_0\dot{\Delta}p_0\right] - \gamma b_2b_3E\left[\Delta p_0\dot{x}_0\right] + \frac{\gamma}{\rho_{\mathrm{atm}}}p^{1/\gamma}_{\mathrm{atm}}E\left[\dot{m}_{\mathrm{turb}}\left(\Delta p_0 + m_{\mathrm{p}} + p_{\mathrm{atm}}\right)^{1-\frac{1}{\gamma}}\right] = 0. \quad (34)$$

Furthermore, the Fourier transforms of the response components are used for computing the associated spectra and cross-spectra as

$$S_{\mathrm{x}_0,\mathrm{x}_0} = |\,\widetilde{X}(\omega)\,|^2, \quad (35)$$

$$S_{\Delta\mathrm{p}_0,\Delta\mathrm{p}_0} = |\,\Delta\widetilde{\mathrm{p}}_0(\omega)\,|^2, \quad (36)$$

and

$$S_{\mathrm{x}_0,\Delta\mathrm{p}_0} = \widetilde{X}(\omega)\,\Delta\widetilde{p}_0{}^*(\omega), \quad (37)$$

where * denotes complex conjugation. Next, employing Eqs. (35)–(37), the corresponding variances are evaluated as

$$\sigma^2_{x_0} = \int_{-\infty}^{\infty} S_{\mathrm{x}_0,\mathrm{x}_0}\mathrm{d}\omega, \quad (38)$$

$$\sigma^2_{\dot{x}_0} = \int_{-\infty}^{\infty} \omega^2 S_{\mathrm{x}_0,\mathrm{x}_0}\mathrm{d}\omega, \quad (39)$$

$$\sigma^2_{\ddot{x}_0} = \int_{-\infty}^{\infty} \omega^4 S_{\mathrm{x}_0,\mathrm{x}_0}\mathrm{d}\omega, \quad (40)$$

$$\sigma^2_{\Delta\mathrm{p}_0} = \int_{-\infty}^{\infty} S_{\Delta\mathrm{p}_0,\Delta\mathrm{p}_0}\mathrm{d}\omega, \quad (41)$$

$$\sigma^2_{\Delta\dot{\mathrm{p}}_0} = \int_{-\infty}^{\infty} \omega^2 S_{\Delta\mathrm{p}_0,\Delta\mathrm{p}_0}\mathrm{d}\omega, \quad (42)$$

and

$$\sigma^2_{\Delta\ddot{\mathrm{p}}_0} = \int_{-\infty}^{\infty} \omega^4 S_{\Delta\mathrm{p}_0,\Delta\mathrm{p}_0}\mathrm{d}\omega, \quad (43)$$

whereas relevant expected values take the form

$$E\left[x_0\Delta p_0\right] = \int_{-\infty}^{\infty} S_{\mathrm{x}_0,\Delta p_0}\mathrm{d}\omega, \quad (44)$$

$$E\left[\dot{x}_0\dot{\Delta}p_0\right] = \int_{-\infty}^{\infty} \omega^2 S_{\mathrm{x}_0,\Delta p_0}\mathrm{d}\omega, \quad (45)$$

$$E\left[x_0\ddot{x}_0\right] = -\int_{-\infty}^{\infty} \omega^2 S_{\mathrm{x}_0,\mathrm{x}_0}\mathrm{d}\omega, \quad (46)$$

$$E\left[x_0\frac{\Delta p^{(\mathrm{D})}}{\rho g}\right]=\frac{1}{\rho g}\int_{-\infty}^{\infty}S_{\mathrm{x}_0,\Delta p^{(D)}}\mathrm{d}\omega, \tag{47}$$

$$E\left[\ddot{x}_0\frac{\Delta p^{(\mathrm{D})}}{\rho g}\right]=-\frac{1}{\rho g}\int_{-\infty}^{\infty}\omega^2 S_{\mathrm{x}_0,\Delta p^{(D)}}\mathrm{d}\omega, \tag{48}$$

$$E\left[x_0\Delta\dot{p}_0\right]=E\left[\dot{x}_0\Delta p_0\right]=\int_{-\infty}^{\infty}\omega S_{\mathrm{x}_0,\Delta p_0}\mathrm{d}\omega \tag{49}$$

and

$$E\left[\mid\dot{x}_0\mid\dot{x}_0^2\right]=\frac{\left(2\sigma_{\dot{x}_0}^2\right)^3\Gamma(3)}{4\sqrt{2\pi}\left(\sqrt{\sigma_{\dot{x}_0}^2}\right)^3}, \tag{50}$$

where Γ denotes the Gamma function [32] and the analytical evaluation of Eq. (50) is provided in Ref. [21]. The remaining expected values appearing in Eqs. (28), (29), (30), (33), (34), are computed numerically by considering the response components to be jointly Gaussian random processes according to the standard statistical linearization assumption. The technique is mechanized as shown in Fig. 2, where it is seen that an iterative scheme is implemented for determining the equivalent coefficients and response statistics. Specifically, the iterations are initiated by setting the equivalent elements equal to values shown in Table 1. Next, the response statistics are obtained and used to update the values of the equivalent coefficients. The iterative procedure continues until convergence of the equivalent elements estimates corresponding to two successive iterations.

4 Numerical example

Numerical results assessing the reliability of the proposed procedure pertain to the case study of the wave power plant built in Civitavecchia (Rome, Italy). Specifically, the results are obtained for a U-OWC chamber with the geometrical characteristics shown in Table 2. The PTO is a Wells turbine [39] with a dimensionless turbine parameter $\Lambda = 0.3$. The rotational speed of the turbine is considered constant and equal to 2800 rpm in all calculations. For computing the converted power, the experimental curves given by Curran and Gato [40] are employed for estimating the turbine efficiency η_{turb}. In this regard, note that the air power available to the turbine is given by the equation

$$P_{\mathrm{available}}=\dot{m}_{\mathrm{turb}}\frac{p_{\mathrm{c}}-p_{\mathrm{atm}}}{\rho_{\mathrm{atm}}}, \tag{51}$$

whereas the expression for the average air power takes the form

$$<P_{\mathrm{available}}>=\frac{\Lambda D}{\Omega\rho_{\mathrm{atm}}}\left(\sigma_{\mathrm{p}}^2+m_{\mathrm{p}}^2\right). \tag{52}$$

Further, the power converted by the turbine is given by

$$P_{\mathrm{turb}}=\eta_{turb}P_{\mathrm{available}}. \tag{53}$$

In this regard, utilizing eqs.(52)–(53), the average power converted by the turbine becomes

$$<P_{\mathrm{turb}}>=\frac{\Lambda D}{\Omega\rho_{\mathrm{atm}}}\int_{-\infty}^{\infty}\left(\Delta p_0+m_{\mathrm{p}}\right)^2\eta_{turb}\,\mathrm{pdf}\left(\Delta p_0\right)\mathrm{d}\Delta p_0, \tag{54}$$

where $\mathrm{pdf}(\Delta p_0)$ is the probability density function of the air pressure fluctuation random process. The coefficients C_{in} and C_{dg} are equal to 0.19 and 0.46, respectively, based on the experimental data in Ref. [31]. Moreover, the reliability of the proposed technique is assessed via comparisons with relevant MC simulation data. For this purpose, a constant average acceleration method is implemented for numerically integrating the equation of motion in the time domain [41], whereas the convolution integral used to account for hydrodynamic memory effects is computed based on a standard trapezoidal integration scheme. To this aim, a time step $dt = 0.01$ s is utilized, whereas the duration of a sea state is $T_0 = 2$ hours. Also, the system excitation is generated by the spectral representation method described in Ref. [42] based on a superposition of 500 harmonics with random phase angles. The derived results pertain to estimated mean values and standard deviations of the various response components, as well as to average air power available to the turbine and average power converted by the turbine. Regarding the excitation process, the U-OWC chamber is subjected to random waves compatible with a JONSWAP power spectrum [43] associated with a significant wave height H_{s} and a peak spectral period T_{p} given by the equation [42]

$$T_{\mathrm{p}}=8.5\pi\sqrt{\frac{H_{\mathrm{s}}}{4g}}. \tag{55}$$

Next, two solution treatments are considered. The first, denoted as "conventional," relates to the solution obtained by ignoring the inlet uncovering as in Refs. [29,30]. The second, denoted as "novel," takes into account the inlet uncovering as described in sections 2 and 3. The relevant outputs are computed for various

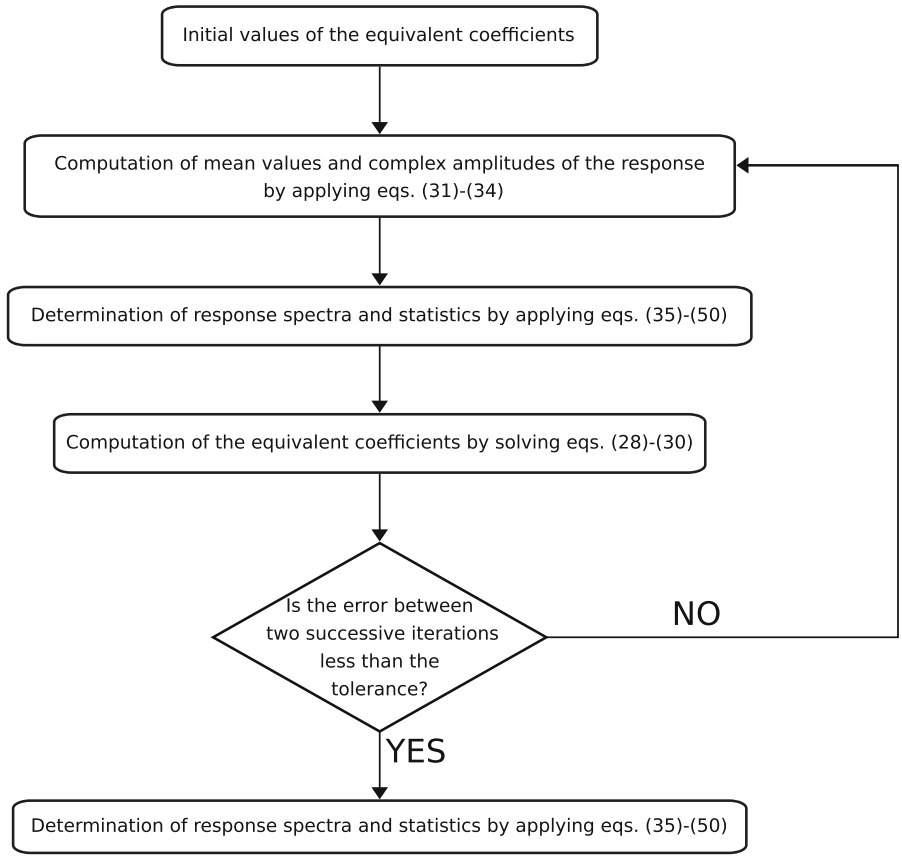

Fig. 2 Flowchart of the mechanization of the technique to obtain the equivalent coefficients and response statistics

Table 1 Initial values of the equivalent coefficients

$M_{eq}^{(1)}$	$K_{eq}^{(1)}$	β_{eq}	$C_{eq}^{(1)}$	$C_{p,eq}^{(2)}$	$C_{x,eq}^{(2)}$	$K_{p,eq}^{(2)}$	$K_{x,eq}^{(2)}$
0	0	1	0	0	0	1	1

Table 2 Geometrical parameters of the U-OWC chamber of the wave power plant of Civitavecchia (Rome, Italy)

d [m]	h [m]	l_i [m]	b_1 [m]	b_2 [m]	b_3 [m]	h_c [m]	D [m]
15	2	5	1.6	3.2	3.87	9.4	0.75

sea states with H_s ranging from 1 m to 4 m. As shown in Fig. 3, the response statistics obtained by the novel statistical linearization technique agree, in general, better with the MC simulation data than the estimates based on the conventional technique. As anticipated, for small values of H_s, the accuracy degrees demonstrated by the conventional and the novel techniques practically coincide. This is due to the fact that inlet uncovering is a rare event. However, for increasing values of H_s, the novel technique is capable of capturing the physics of the problem better, and thus, it exhibits a higher accuracy degree than the conventional technique. Further, note that, for the most severe sea states, the standard deviations of the response quantities corresponding to the novel technique are smaller than the ones obtained by the conventional treatment. This can be attributed to the fact that in such sea states individual wave heights are larger, in general, than in mild sea states. Therefore, they are more likely to uncover the U-OWC inlet.

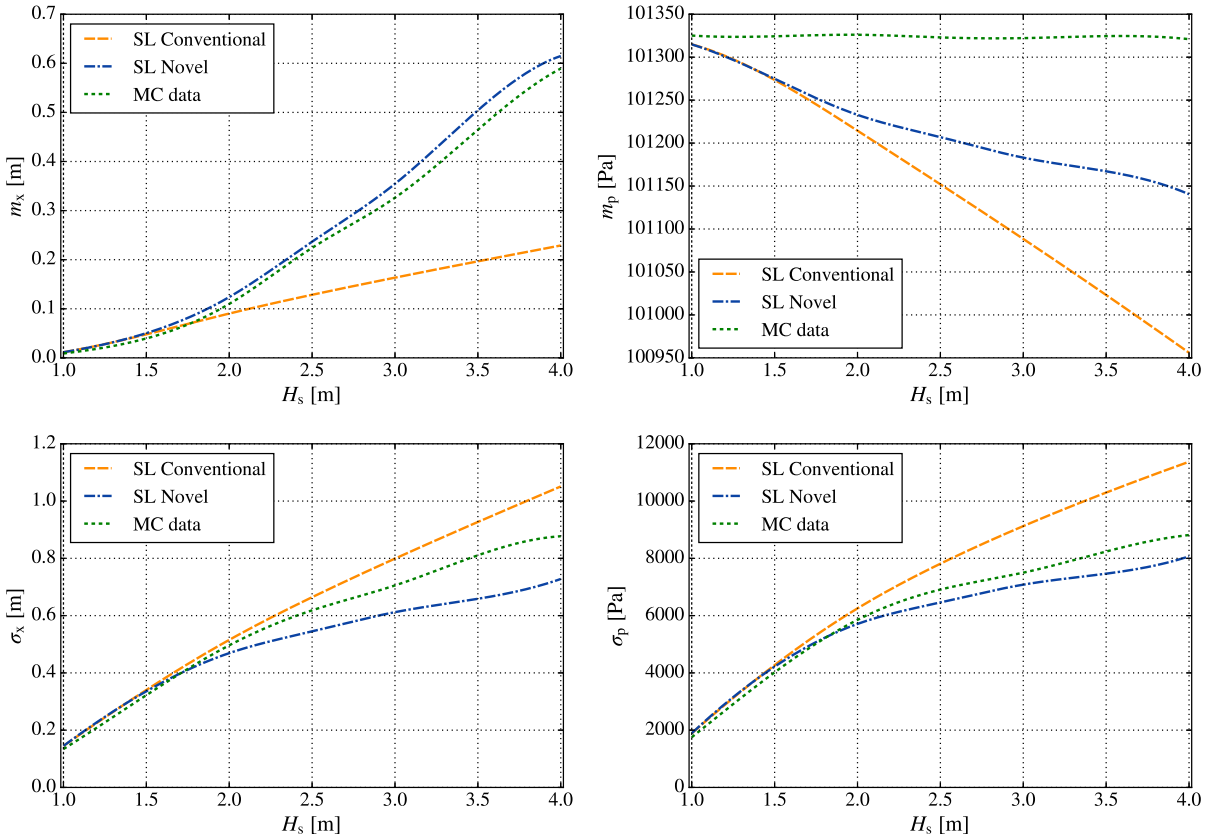

Fig. 3 Comparison between statistical linearization (SL) and Monte Carlo (MC) outputs. Mean values (top panels) and standard deviations (bottom panels) of the oscillating water column displacement (left panels) and of the air pressure fluctuation (right panels) for a given significant wave height H_s

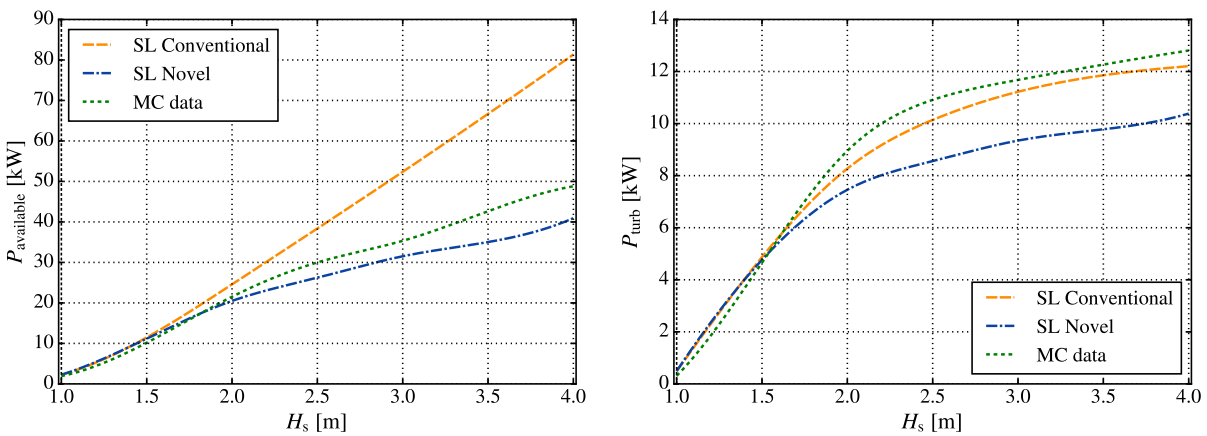

Fig. 4 Comparison between statistical linearization (SL) and Monte Carlo (MC) results of the air power in the chamber and of the power converted by the Wells turbine as a function of the significant wave height H_s. Results are obtained for a depth of the U-duct opening of $h = 2$ m

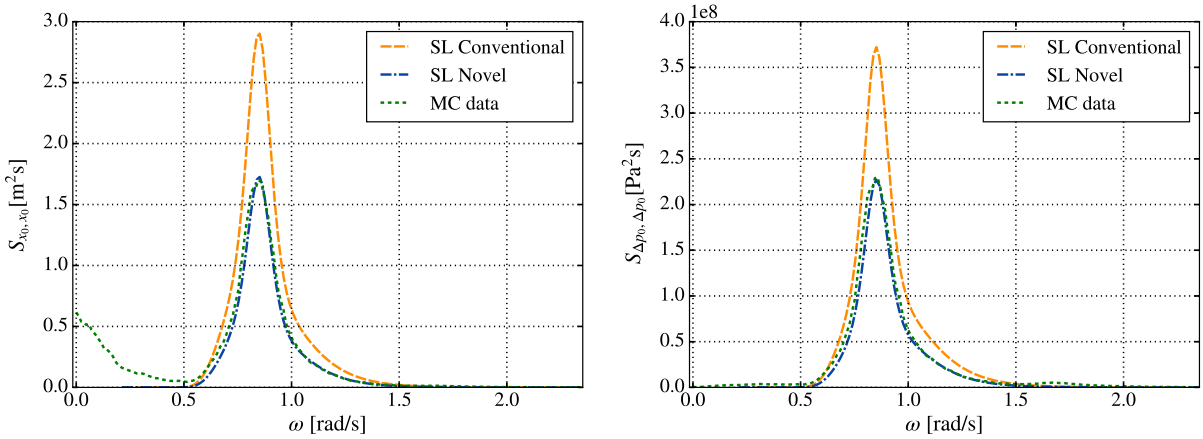

Fig. 5 Power spectra of the water column displacement (left panel) and of the air pressure (right panel) of the U-OWC chamber with the opening of the U-duct located at $h = 2$ m below the mean water level. The device is excited by a sea state with $H_s = 3$ m

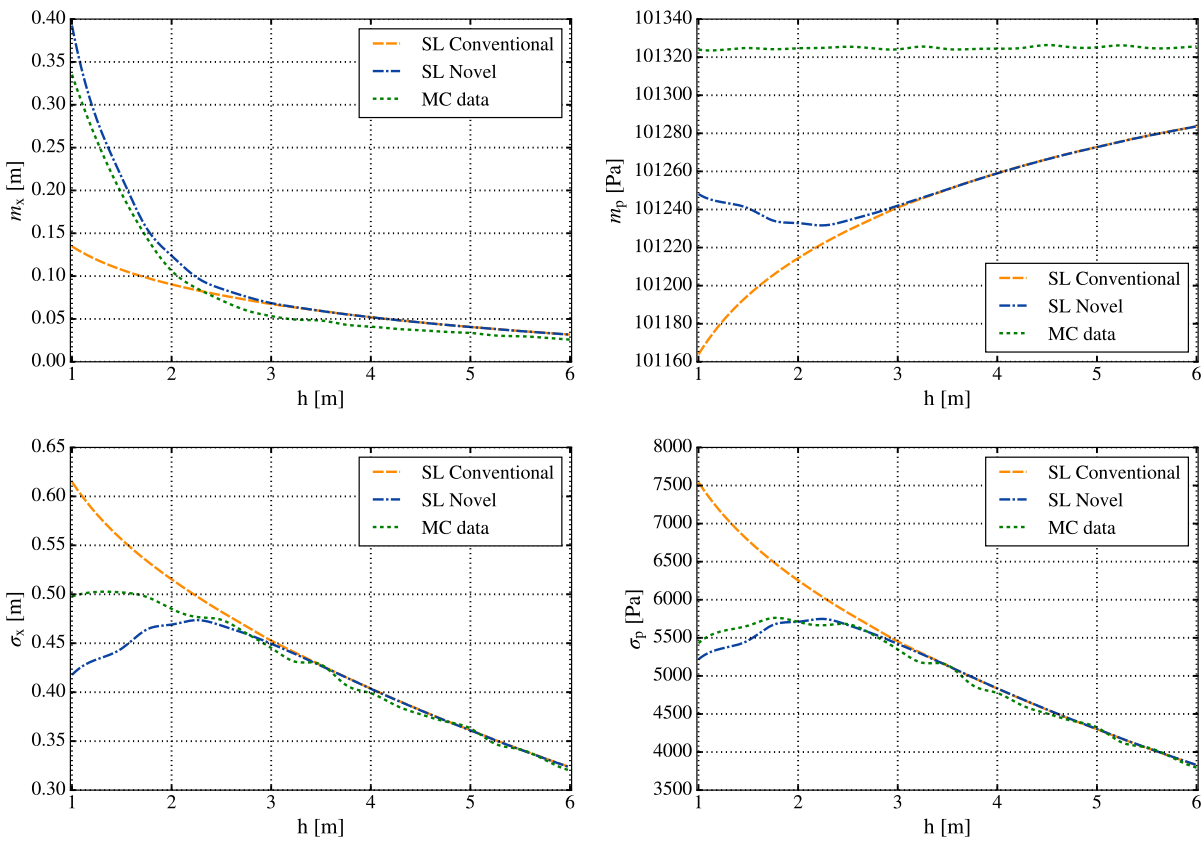

Fig. 6 Comparison between statistical linearization (SL) and Monte Carlo (MC) results. Mean values (top panels) and standard deviations (bottom panels) for given submergence depth values h of the U-duct. Results are obtained for a sea state with $H_s = 2$ m

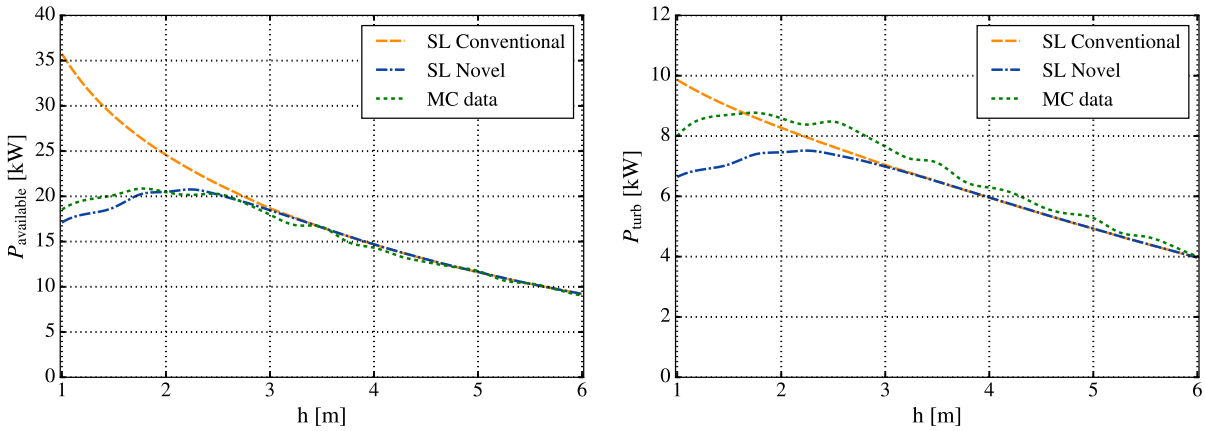

Fig. 7 Comparison between statistical linearization (SL) and Monte Carlo (MC) data. Available air power (left panel) and converted power (right panel) for given submergence depth values h of the U-duct opening. Results pertain to a sea state with $H_s = 2\,\text{m}$

Similar conclusions can be drawn for available and converted air power based on data shown in Fig. 4. In particular, although the novel statistical linearization solution underestimates systematically the MC-based data, it appears capable of identifying successfully the salient features and the basic trends of the response statistics and power outputs. This aspect in conjunction with the high computational efficiency render the novel technique an indispensable tool to be used for preliminary design applications. In contrast, the available power in the conventional statistical linearization treatment shows a monotonically increasing behavior. This is due to the fact that it does not account for the inlet uncovering effect.

Further, the power spectra of the water column displacement and of the air pressure of the U-OWC chamber are determined and plotted in Fig. 5. The numerical results are obtained for a sea state with $H_s = 3\,\text{m}$. The comparisons with pertinent MC data indicate a high degree of accuracy exhibited by the novel technique in capturing the frequency contents of the response processes. Although the conventional technique captures the frequency content satisfactorily, it significantly overestimates the magnitudes of the power spectra.

It is clearly seen that accounting for inlet uncovering does play an important role in the computation of response statistics and power outputs. In this context, the impact of the submergence depth h is significant. Indeed, a relatively small submergence depth increases the uncovering time duration, thus reducing the power output. Further, increasing the inlet submergence depth reduces the excitation amplitude, which leads to reducing the power output as well. The impact of the submergence depth h is investigated in Fig. 6, where the technique is applied by varying h for a sea state with $H_s = 2\,\text{m}$. The novel statistical linearization results agree reasonably well with the corresponding MC simulations. Clearly, the largest discrepancies are observed at $h = 1\,\text{m}$, where uncovering is more frequent. Nevertheless, note that the discrepancies for the novel treatment are relatively small taking into account that there is approximately 0.06 m difference in the m_x values and 80 Pa in the m_p values. Similar trends can be observed in the standard deviations, where the discrepancies decrease by increasing the depth of the U-duct opening. For values larger than $h = 2.5\,\text{m}$, the two solution treatments yield practically identical results due to the fact that the uncovering time duration is negligible. The σ_p plot shows an optimum value at approximately $h = 2\,\text{m}$. This pattern can be observed also in Fig. 7, which shows the air power available to the turbine and the power converted by the turbine. These plots show that the novel statistical linearization solutions are in satisfactory agreement with the results obtained by MC simulations. It is noted that they systematically underestimate MC-based estimates, particularly in cases where the uncovering event is more frequent.

Further, regarding the novel concept of the equivalent coefficient β_{eq}, it is seen in Fig. 8 that it decreases considerably ($\beta_{eq} < 1$) for relatively small values of submergence depth h. This is anticipated since for decreasing depth h the uncovering event is more fre-

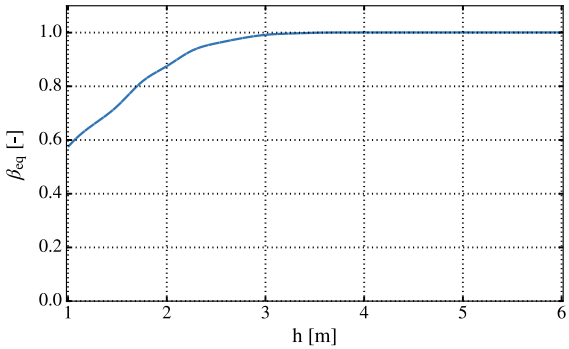

Fig. 8 Equivalent coefficient, β_{eq}, as a function of the position, h, of the U-duct opening below the mean water level. A sea state with $H_s = 2$ m is considered

quent and the intermittent nature of the excitation becomes more prevalent. Furthermore, in agreement with the physics of the problem, for relatively large values of h, β_{eq} converges to 1 corresponding to uninterrupted, constantly applied, excitation.

5 Concluding remarks

In this paper, a novel statistical linearization technique has been developed for determining approximately the response statistics and the power output of U-OWC energy harvesting systems. Specifically, first, a mathematical model has been derived for describing the governing dynamics of the harvester by employing the unsteady Bernoulli equation. This has led to a coupled system of nonlinear integro-differential stochastic equations. A novel aspect of the governing equations relates to the fact that the intermittent, i.e., nonstationary, nature of the wave excitation, occurring in severe sea states due to uncovering of the U-OWC inlet, has been explicitly accounted for. This has been done by multiplying the excitation process with a Heaviside function dependent on the instantaneous free surface displacement. Further, first- and second-order response statistics have been determined approximately by relying on a statistical linearization solution treatment of the problem. In this regard, the original system of nonlinear equations has been replaced by an equivalent linear one, whose parameters have been obtained by minimizing the mean square error between the two systems. Note that the Heaviside function has also been replaced in the equivalent linear system by an equivalent excitation coefficient. Compared with earlier research efforts in the literature that relied on statistical linearization, it has been shown herein that the developed technique providing also an equivalent excitation coefficient yields an enhanced accuracy degree. In fact, the technique can be construed as a direct generalization of the conventional statistical linearization, since setting the excitation coefficient equal to one leads to the standard implementation of the scheme.

The U-OWC installed in the Civitavecchia harbor (Rome, Italy) has been considered as an illustrative numerical example. In this regard, the response statistics and the power outputs estimated by the developed approximate technique have been compared with pertinent Monte Carlo simulation data. It has been shown that the statistical linearization technique exhibits a satisfactory degree of accuracy in determining the response statistics and power outputs, and appears capable of capturing the salient characteristics of relevant response power spectra as well. Overall, it can be argued that the aspect of yielding conservative estimates by systematically underestimating the power output, in conjunction with the high computational efficiency, renders the novel technique a potent tool to be used for preliminary design applications.

Author contributions A. Scialò contributed to conceptualization, methodology, software, and writing–original draft. G. Malara contributed to conceptualization, methodology, and writing–review and editing. I. A. Kougioumtzoglou contributed to conceptualization, methodology, and writing–review and editing. F. Arena contributed to funding acquisition, resources, and writing–review and editing.

Funding Open access funding provided by Universitá degli Studi Mediterranea di Reggio Calabria within the CRUI-CARE Agreement. The activity of Dr. Andrea Scialò was funded through the scholarship *Supporto all'attività sperimentale nel laboratorio NOEL nell'ambito del progetto Horizon 2020 denominato "The Blue Growth Farm"* by the project "The Blue Growth Farm".

Code availability Data including the codes will be made available on request.

Declarations

Conflict of interest The authors declare that they have no conflict of interest.

References

1. Falcão, A.F. de O.: Wave energy utilization: a review of the technologies. Renew. Sustain. Energy Rev. **14**(3), 899–918 (2010). https://doi.org/10.1016/j.rser.2009.11.003
2. Torre-Enciso, Y., Ortubia, I., López de Aguileta, L.I.I., Marqués, J.: Mutriku wave power plant: from the thinking out to the reality. In: Proceedings of 8th European Wave Tidal Energy Conf, Uppsala, Sweden, pp. 319–329 (2009)
3. Li, L., Ruzzo, C., Collu, M., Gao, Y., Failla, G., Arena, F.: Analysis of the coupled dynamic response of an offshore floating multi-purpose platform for the Blue Economy. Ocean Eng. **217**, 107943 (2020). https://doi.org/10.1016/j.oceaneng.2020.107943
4. Wells, A.A.: Fluid driven rotary transducer, British Patent Spec. No 1595700 (1976)
5. Falcão, A.F.O., Gato, L.M.C., Nunes, E.P.A.S.: A novel radial self-rectifying air turbine for use in wave energy converters. Renew. Energy **50**, 289–298 (2013). https://doi.org/10.1016/j.renene.2012.06.050
6. Rezanejad, K., Bhattacharjee, J., Guedes Soares, C.: Stepped sea bottom effects on the efficiency of nearshore oscillating water column device. Ocean Eng. **70**, 25–38 (2013). https://doi.org/10.1016/j.oceaneng.2013.05.029
7. Rezanejad, K., Souto-Iglesias, A., Guedes Soares, C.: Experimental investigation on the hydrodynamic performance of an L-shaped duct oscillating water column wave energy converter. Ocean Eng. **173**, 388–398 (2019). https://doi.org/10.1016/j.oceaneng.2019.01.009
8. Boccotti, P.: On a new wave energy absorber. Ocean Eng. **30**(9), 1191–1200 (2003). https://doi.org/10.1016/S0029-8018(02)00102-6
9. Boccotti, P.: Comparison between a U-OWC and a conventional OWC. Ocean Eng. **34**(5), 799–805 (2007). https://doi.org/10.1016/j.oceaneng.2006.04.005
10. Fox, B.N., Gomes, R.P.F., Gato, L.M.C.: Analysis of oscillating-water-column wave energy converter configurations for integration into caisson breakwaters. Appl. Energy **295**, 117023 (2021). https://doi.org/10.1016/j.apenergy.2021.117023
11. Scialò, A., Malara, G., Arena, F.: Geometrical optimization of U-Oscillating Water Columns in random waves. In: Proceedings of the 38th International Conference on Ocean, Offshore and Arctic Engineering, OMAE 2019, Glasgow, Scotland, UK (2019). https://doi.org/10.1115/OMAE2019-95973
12. Ning, D., Baoming, G., Rongquan, W., Vyzikas, T., Greaves, D.: Geometrical investigation of a U-shaped oscillating water column wave energy device. Appl. Ocean Res. **97**, 102105 (2020). https://doi.org/10.1016/j.apor.2020.102105
13. Scialò, A., Henriques, J.C.C., Malara, G., Falcão, A.F.O., Gato, L.M.C., Arena, F.: Power take-off selection for a fixed U-OWC wave power plant in the Mediterranean Sea: the case of Roccella Jonica. Energy **215**, 119085 (2021). https://doi.org/10.1016/j.energy.2020.119085
14. Moretti, G., Scialò, A., Malara, G., Muscolo, G.G., Arena, F., Vertechy, R., Fontana, M.: Hardware-in-the-loop simulation of wave energy converters based on dielectric elastomer generators. Meccanica **56**, 1223–1237 (2021). https://doi.org/10.1007/s11012-021-01320-8
15. Boccotti, P.: Caisson breakwaters embodying an OWC with a small opening-Part I: theory. Ocean Eng. **34**(5), 806–819 (2007). https://doi.org/10.1016/j.oceaneng.2006.04.006
16. Malara, G., Arena, F.: Response of U-oscillating water column arrays: semi-analytical approach and numerical results. Renew. Energy **138**, 1152–1165 (2019). https://doi.org/10.1016/j.renene.2019.02.018
17. Psaros, A.F., Brudastova, O., Malara, G., Kougioumtzoglou, I.A.: Wiener Path Integral based response determination of nonlinear systems subject to non-white, non-Gaussian, and non-stationary stochastic excitation. J. Sound Vib. **433**, 314–333 (2018). https://doi.org/10.1016/j.jsv.2018.07.013
18. Petromichelakis, I., Kougioumtzoglou, I.: Addressing the curse of dimensionality in stochastic dynamics: a Wiener path integral variational formulation with free boundaries. Proc. R. Soc. A **476**, 20200385 (2020). https://doi.org/10.1098/rspa.2020.0385
19. Petromichelakis, I., Psaros, A.F., Kougioumtzoglou, I.A.: Stochastic response determination and optimization of a class of nonlinear electromechanical energy harvesters: a Wiener path integral approach. Probab. Eng. Mech. **53**, 116–125 (2018). https://doi.org/10.1016/j.probengmech.2018.06.004
20. Petromichelakis, I., Psaros, A., Kougioumtzoglou, I.: Stochastic response analysis and reliability-based design optimization of nonlinear electromechanical energy harvesters with fractional derivative elements. ASCE-ASME J. Risk Uncertainty Eng. Syst. Part B: Mech. Eng. **7**(1) (2021). https://doi.org/10.1115/1.4049232
21. Roberts, J.B., Spanos, P.D.: Random Vibration and Statistical Linearization. Dover Publications (2003). https://store.doverpublications.com/0486432408.html
22. Socha, L.: Linearization Methods for Stochastic Dynamic Systems. Springer Berlin, Heidelberg (2008). https://doi.org/10.1007/978-3-540-72997-6
23. Spanos, P., Kougioumtzoglou, I.: Harmonic wavelets based statistical linearization for response evolutionary power spectrum determination. Probab. Eng. Mech. **27**(1), 57–68 (2012). https://doi.org/10.1016/j.probengmech.2011.05.008
24. Kougioumtzoglou, I.A., Spanos, P.D.: Harmonic wavelets based response evolutionary power spectrum determination of linear and non-linear oscillators with fractional derivative elements. Int. J. Non-Linear Mech. **80**, 66–75 (2016). https://doi.org/10.1016/j.ijnonlinmec.2015.11.010
25. Kougioumtzoglou, I., Fragkoulis, V., Pirrotta, A.: Random vibration of linear and nonlinear structural systems with singular matrices: A frequency domain approach. J. Sound Vib.

404, 84–101 (2017). https://doi.org/10.1016/j.jsv.2017.05.038
26. Silva, L.S.P., Sergiienko, N.Y., Pesce, C.P., Ding, B., Cazzolato, B., Morishita, H.M.: Stochastic analysis of nonlinear wave energy converters via statistical linearization. Appl. Ocean Res. **95**, 102023 (2020). https://doi.org/10.1016/j.apor.2019.102023
27. Silva, L.S.P., Morishita, H., Pesce, C., Gonçalves, R.: Nonlinear analysis of a heaving point absorber in frequency domain via statistical linearization. In: Proceedings of the 38th International Conference on Ocean, Offshore and Arctic Engineering, OMAE 2019 (2019). https://doi.org/10.1115/OMAE2019-95785
28. Silva, L.S.P., Pesce, C., Morishita, H., Gonçalves, R.: Nonlinear analysis of an oscillating water column wave energy device in frequency domain via statistical linearization. In: Proceedings of the 38th International Conference on Ocean, Offshore and Arctic Engineering, OMAE 2019 (2019). https://doi.org/10.1115/OMAE2019-96727
29. Malara, G., Spanos, P.D.: Efficient determination of nonlinear response of an array of Oscillating Water Column energy harvesters exposed to random sea waves. Nonlinear Dyn. **98**(3), 2019–2034 (2019). https://doi.org/10.1007/s11071-019-05303-z
30. Spanos, P.D., Strati, F.M., Malara, G., Arena, F.: An approach for non-linear stochastic analysis of U-shaped OWC wave energy converters. Probab. Eng. Mech. **54**, 44–52 (2018). https://doi.org/10.1016/j.probengmech.2017.07.001
31. Arena, F., Romolo, A., Malara, G., Fiamma, V., Laface, V.: Validation of the U-Oscillating Water Column model by full-scale experimental data. In: Proceedings of the 12th European Wave and Tidal Energy Conference, Cork, Ireland, pp. 1038-1–1038-5 (2017)
32. Abramowitz, M., Stegun, I.A., Romer, R.H.: Handbook of mathematical functions with formulas, graphs, and mathematical tables. Am. J. Phys. **56**(10), 958–958 (1988). https://doi.org/10.1119/1.15378
33. Falcão, A.F.O., Henriques, J.C.C.: The spring-like air compressibility effect in oscillating-water-column wave energy converters: review and analyses. Renew. Sustain. Energy Rev. **112**, 483–498 (2019). https://doi.org/10.1016/j.rser.2019.04.040
34. Falcão, A.F. de O., Rodrigues, R.: Stochastic modelling of OWC wave power plant performance. Appl. Ocean Res. **24**(2), 59–71 (2002). https://doi.org/10.1016/S0141-1187(02)00022-6
35. Spanos, P.D., Iwan, W.D.: Harmonic analysis of dynamic systems with nonsymmetric nonlinearities. J. Dyn. Syst. Meas. Control. **101**(1), 31–36 (1979). https://doi.org/10.1115/1.3426393
36. Mei, C.C., Stiassnie, M., Yue, D.K.K.: Theory and Applications of Ocean Surface Waves. World Scientific, Singapore (2005)
37. Young, G.E., Chang, R.J.: Prediction of the response of nonlinear oscillators under stochastic parametric and external excitations. Int. J. Non-Linear Mech. **22**(2), 151–160 (1987). https://doi.org/10.1016/0020-7462(87)90017-5
38. Chang, R.J., Young, G.E.: Methods and Gaussian criterion for statistical linearization of stochastic parametrically and externally excited nonlinear systems. ASME. J. Appl. Mech. **56**(1), 179–185 (1989). https://doi.org/10.1115/1.3176042
39. Raghunathan, S.: The wells air turbine for wave energy conversion. Prog. Aerosp. Sci. **31**(4), 335–386 (1995). https://doi.org/10.1016/0376-0421(95)00001-F
40. Curran, R., Gato, L.M.C.: The energy conversion performance of several types of Wells turbine designs. Proc. Inst. Mech. Eng. Part A: J. Power Energy **211**(2), 133–145 (1997). https://doi.org/10.1243/0957650971537051
41. Clough, R.W., Penzien, J.: Dynamics of Structures. Computers Structures Inc, Berkeley (1995)
42. Boccotti, P.: Wave Mechanics and Wave Loads on Marine Structures. Butterworth-Heinemann, Oxford (2015)
43. Hasselmann, K., Barnett, T., Bouws, E., Carlson, H., Cartwright, D., Enke, K., Ewing, J., Gienapp, H., Hasselmann, D., Kruseman, P., Meerburg, A., Muller, P., Olbers, D., Richter, K., Sell, W., Walden, H.: Measurements of wind-wave growth and swell decay during the Joint North Sea Wave Project (JONSWAP). Deut. Hydrogr. Z. **8**, 1–95 (1973)